Desalination and Water Treatment
www.deswater.com

doi: 10.5004/dwt.2020.25412

185 (2020) 226–236
May

Biosorption of heavy metal ions on peel of *Artocarpus nobilis* fruit: 2. Improvement of biosorption capacities of Ni(II) through different modifications

Prasanna Anurudda Kotabewatta[a,b], Namal Priyantha[a,b,*], Linda B.L. Lim[c]

[a]*Postgraduate Institute of Science, University of Peradeniya, Peradeniya, Sri Lanka, emails: namal.priyantha@yahoo.com (N. Priyantha), prasannaanurudda@yahoo.com (P.A. Kotabewatta)*
[b]*Department of Chemistry, University of Peradeniya, Peradeniya, Sri Lanka*
[c]*Department of Chemistry, Faculty of Science, University Brunei Darussalam, Gadong, Brunei Darussalam, email: linda.lim@ubd.edu.bn (L.B.L. Lim)*

Received 17 July 2019; Accepted 4 January 2020

ABSTRACT

Processing of raw fruit peel ($0.71 < d < 1$ mm) of *Artocarpus nobilis* biosorbent using distilled water-washed peel (DWP), and modification with aqueous NaOH solutions (STP) of different concentrations enhances the extent of removal of Ni(II) as a result of increase in surface negative charges, porous nature and the mass to volume ratio. An increase in surface negativity is contributed by deprotonation of functional groups present in the biosorbent, and the cleavage of esters through saponification during the NaOH treatment. The surface area of the biosorbent is increased by breaking down of structural materials, such as lignin, during base treatment. The specific surface areas of DWP, and STP prepared by treatment with 0.10 M NaOH are 381.90 and 919.01 $m^2 g^{-1}$, respectively. The high surface area of STP is convinced by observing small cavities in scanning electron microscopy images. The optimum shaking and settling times are recorded as 2.0 h and 15 min, respectively, for both DWP and STP, while the ambient pH of Ni(II) solutions 5.0 leads to the maximum removal. Under these conditions, the maximum removal of 14.925 mg g^{-1} is obtained for STP3 from synthetic solutions at ambient solution temperature without any thermal treatment of the biosorbent. An important aspect of this biosorbent is that, although thermal treatment of DWP enhances its biosorption capacity, STP provides even higher capacity without any thermal treatment.

Keywords: *Artocarpus nobilis*; Modification; NaOH; Adsorption isotherm; Kinetics models; Intraparticle diffusion model

1. Introduction

Adverse effects of high heavy metal consumption in developing countries have been on the increase due to improper use of hazardous chemicals and poor waste management practices [1]. Further, rapid industrialization and urbanization approaches have undoubtedly contributed to increased levels of heavy metals in the environment. Consequently, aquatic fauna and flora experience this unhealthy, toxic situation through biomagnification. Among many types of industrial pollutants, heavy metal pollution in developing countries is significantly contributed by the high usage of Ni(II) [2,3]. Nickel is the most important metal in the industrial sector for Ni plating, colored ceramics, batteries, furnaces and alloys. Discharging of Ni(II) containing wastewater to the environment could cause harmful effects on the ecosystem and human health [4]. Further, Ni(II) has been identified as a primary pollutant due to its high mobility in water bodies [5]. According to the WHO guidelines, the maximum permissible limit of Ni in drinking water is 0.02 mg L^{-1} [6]. A decrease in Ni(II) levels in contaminated water below its permissible limits are thus necessary before

---

* Corresponding author.

it is disposed off. Among various conventional wastewater treatment techniques applied in the industrial sector, a new trend has been to use adsorption processes for the removal of heavy metal ions and their compounds present in water [7].

Plant-based materials are rich in cellulose, hemicellulose, and lignin, and the composition of these compounds depends on the plant part, such as leaves, seeds, stem, fruits, bark, and roots, and further, it varies from plant species to species. These compounds act as structural materials for higher plants [8]. Owing to the availability of electronegative functional groups present in the above compounds, plant materials show affinity toward heavy metal ions dissolved in water, thereby showing biosorption characteristics. Although biosorption exhibits advantages, such as environmentally friendliness, low-cost and readily availability, the efficiency of biosorption toward heavy metals may not be as high as that of chemical treatment, which has become a limiting factor for the application of biosorbents in the field of industrial effluent treatment. This drawback can be remedied through chemical modification of biosorbents with the aid of relatively nontoxic chemicals for efficient enhancement. Modification of biosorbents would generate new surfaces, and hence, chemical characteristics of the biosorbent could be significantly changed, acting as an adsorbent with novel characteristics. An attractive feature of chemical modification is that selectivity of contaminant removal could be achieved through proper selection of the modifier, based on its known properties. For instance, the chelating ability could be enhanced through ethylenediaminetetraacetic acid (EDTA) treatment, and hydrolysis of ester linkages could be favored through acid or base treatment. Biosorbents modified with a strong base, such as NaOH, have shown remarkable advantages as compared to other modifying agents [9]. In addition to the saponification of esters leading to an increase in metal ion sorption capacities, lignocellulosic materials in the biosorbent can be swelled by absorbing water, increasing the internal surface area forming new cavities and porous nature [10,11]. The additional advantages are the decrease in the degree of polymerization, crystallinity, breakdown of linkage of lignin and carbohydrate and destruction of lignin structure [9].

The above area of research has recently been addressed; however, chemically modified biosorbents for the treatment of real industrial effluents are still at the infant stage. In this context, the present study is on the enhancement of adsorption characteristics of the peel of *Artocarpus nobilis* fruit using two approaches: treatment with distilled water; and modification with diluted NaOH solutions. This plant species is included in genus *Artocarpus* and is endemic to Sri Lanka, and the peel of matured and ripened fruits was used for the research activity. A comparison of biosorption characteristics of raw peel, distilled water-washed peel (DWP), and NaOH-treated peel (STP) toward Ni(II) under optimized conditions is also reported. Applications of kinetics, adsorption isotherm models and intraparticle diffusion (IPD) model for the interaction of Ni(II) on DWP and STP have also been elaborated.

The fruit of *Artocarpus* species is rich in carboxylic acids and its derivatives. For instance, Jackfruit, which belongs to *Moraceae* family, consists of varieties of fatty acids of capric, arachidic, myristic, palmitic, oleic, stearic, lauric and linoleic [12]. The fruit peel of *Artocarpus nobilis* consists of organic functional groups, such as carboxylic acids and its derivatives, including ester, alcohol and phenolic compounds. Further, the Point of Zero Charge of the peel of *Artocarpus nobilis* has been estimated within the pH of 3.0–4.5, and the surface charge of the peel is negative within the pH range of 4.0–10.0 [13]. The heavy metal ion, Ni(II), shows a high affinity to organic functional groups present in cell walls, such as organic acids and its derivatives, phenolic compounds, and amide groups providing attractive forces for biosorption of heavy metal ions [14,15]. In addition, the porous nature of the biosorbent is another advantage for metal ion removal through biosorption.

Considering the above aspects, the main objective of this research was to enhance the adsorption capacity of the fruit peel of *Artocarpus nobilis* for the removal of Ni(II) from aqueous synthetic solutions. Surface modification of the biosorbent was achieved through treatment with distilled water or diluted NaOH solutions. In addition, the effect of change in processing conditions (temperature, concentration) of the modifying agent on the biosorption capacity toward Ni(II) was also considered for identifying optimum conditions for the most efficient removal.

2. Material and methods

2.1. Sample preparation

The matured and ripened fruits of *Artocarpus nobilis* were collected from Kandy District in Sri Lanka. Fruits collected were washed thoroughly with tap water for removing dust, solid and sand particles. Thereafter, the outer peel of fruits was removed and allowed to air dry under ambient conditions. Dried peel was thoroughly mixed, sieved using 1.0 and 0.71 mm sieves, and one portion of the samples of diameter in the range of $0.71 < d < 1.0$ mm was washed thoroughly with distilled water until a clear supernatant was obtained. Thereafter, the above portion of the peel was air-dried for further experiments. Another portion of the peel was modified using NaOH solutions of 0.01, 0.05, 0.10 and 0.15 M concentrations. These NaOH-treated peels (STP) types were labeled as STP1, STP2, STP3 and STP4, respectively. For modification; 50.0 g of raw peel was mixed with 1.0 L of NaOH solution of each concentration and stirred for 1.0 h followed by 24 h settling. Then, NaOH solution was drained out and the excess base was removed using tap water, followed by distilled water. Modified peel was continuously washed with excess distilled water until the pH of the supernatant was matched with that of distilled water. Modified peel was air-dried for subsequent experiments. The above procedure was extracted from elsewhere and modified as needed for this research [16,17].

2.2. Instrumentation

Spectro-electronic Thermo M series atomic absorption spectrophotometer (AAS) was used to measure the total concentration of Ni(II) in solution. Metals present in biosorbent samples were determined using X-ray fluorescence (XRF) spectrophotometer (Fischerscope Model-DF500FG-456). Surface titration experiments were conducted with digital pH meter (Orion Model 960, USA) while scanning electron microscopy (SEM) images were taken using Oxford Instruments – EVO LS 15 (Zeiss) instrument, Germany. Fourier-transform infrared (FTIR) spectra were recorded on Thermo Nicolet Model-Avatar 320 FTIR spectrophotometer for identification of organic functional groups, while UV/Vis spectrophotometer (Shimadzu UV 1800 series, Japan) was used in order to determine the concentrations of colored species.

2.3. Chemicals

Analytical grade chemicals were used for the preparation of all reagents. A stock solution of 1,000 mg L^{-1} Ni(II) was prepared using $NiNO_3$ (Sigma-Aldrich, Germany) in distilled water. All standards of Ni(II) were prepared using the stock solution. The preparation of solutions of different pHs was done using 0.10 M NaOH and 0.10 M HNO_3. Methylene blue (MB) and KBr were purchased from Sigma-Aldrich. A stock solution of 2,000 mg L^{-1} MB was prepared by dissolving MB in distilled water. All chemicals were used without further purification.

2.4. Methods

2.4.1. FTIR and SEM analysis

Powdered biosorbent (d < 0.063 mm) samples were analyzed on the FTIR spectrophotometer using the KBr pellet method [18]. Microscopic biosorption sites and the surface appearance of the biosorbent were investigated through SEM images.

2.4.2. Determination of specific surface area

A sample of 2.00 g of MB dye was dissolved in 1,000.0 mL DI water to prepare a stock solution of 2,000 mg L^{-1}, which was then used to prepare a series of standard solutions. A sample of 0.100 g of DWP was shaken with 50.0 mL of MB and allowed to mix for 2.0 h, and the mixture was allowed to stand overnight. A 5.00 mL aliquot of the supernatant was removed and centrifuged. The concentration of MB in the supernatant was determined at the λ_{max} of 662 nm [19]. The same procedure was followed for MB solutions of different concentrations. Then, the experiment was repeated for STP3 using the same procedure.

2.4.3. XRF analysis

Raw biosorbent sample was shaken with 50.0 mL of 1,000 mg L^{-1} Ni(II) solution at 150 rpm for 60 min. Then, the suspension was filtered and dried. Dried samples of Ni-sorbed biosorbent and respective raw peel, DWP and STP3 samples were used for XRF analysis.

2.4.4. Optimization of contact time

The effect of contact time on biosorption was observed by varying shaking and settling times separately. For optimization of shaking time, 50.0 mL aliquot of 10.0 mg L^{-1} Ni(II) solution was thoroughly shaken with 0.100 g of biosorbent for different shaking times from 0 to 180 min, followed by zero settling time. The extent of removal at different shaking times was calculated to determine the optimum shaking time. After optimization of shaking time, similar experiments were carried out to optimize settling time (waiting time) by employing optimized shaking time, for different settling times from 0 to 75 min.

2.4.5. Optimization of heating time

Representative samples of DWP, STP1, STP2, STP3 and STP4 were heated for different time periods under a predetermined constant temperature of 125°C. In each experiment, 50.0 mL of each Ni(II) solution (10.0 mg L^{-1}) was mixed with 0.100 g of preheated biosorbent, and the extent of removal was determined under the optimized contact times. The extent of removal at different treatment time periods was calculated to determine the optimum heating time.

2.4.6. Optimization of treatment temperature

Biosorbent samples (DWP, STP1, STP2, STP3, and STP4) were heat-treated at predetermined temperatures in the range from 60°C to 225°C at the respective optimized heating time and the extent of Ni(II) removal was determined. For this purpose, 50.0 mL aliquots of Ni(II) solution (10.0 mg L^{-1}) was mixed with 0.100 g of each of the above biosorbents, and optimized contact times were applied. The extent of removal of Ni(II) at different treatment temperature was calculated for each sample to determine the optimum temperature of the treatment of the biosorbent.

2.4.7. Optimization of pH

Solutions of 10.0 mg L^{-1} Ni(II) having pH ranging from 1–7 were prepared using HNO_3 and NaOH solutions. Solutions of higher pH were not used as precipitation problems were encountered. Each solution was then treated with biosorbents (DWP, STP1, STP2, STP3 and STP4) under the optimum experimental conditions, and the extent of removal was calculated at different pHs to determine the optimum pH.

2.4.8. Adsorption isotherms modeling

The amount of Ni(II) adsorbed on the modified peel (DWP, STP1, STP2, STP3 and STP4) for previously optimized experimental conditions was studied using solutions of concentration varying from 10–1,000 mg L^{-1}. After each solution was filtered, atomic absorption measurements were recorded. The extent of biosorption was calculated as the mass of Ni(II) adsorbed (in mg) on 1.0 g of biosorbent. These data were fitted to the Langmuir and Freundlich adsorption isotherm models.

2.4.9. Adsorption kinetics

To investigate the validity of kinetics models, 500 mL of 10.0 mg L^{-1} solutions of Ni(II) was stirred with 1:100 (w/v) of DWP and STP3. After every 1.0 min interval, samples were withdrawn for the first 15 min period, and thereafter, sampling was done after 5 min intervals up to 60 min. Samples withdrawn were immediately filtered and the remaining concentration of Ni(II) was determined using AAS. The data obtained in these experiments were used for the investigation of the order of reaction by applying kinetics and diffusion models, such as pseudo-first-order (PFO) and pseudo-second-order (PSO) kinetics, and the intra-particle diffusion (IPD) model.

3. Results and discussion

3.1. Characterization of biosorbent

3.1.1. FTIR analysis

The FTIR spectrum, given in Fig. 1, shows a number of organic functional groups present in STP3. The prominent bands are shown at the wavenumbers of 1,629; 1,733; 2,850; 2,917; and 3,330 cm^{-1}. The functional groups present in STP3 corresponding to these wavenumbers, shown in Table 1, would contribute to uptake Ni(II) from aqueous solution. Waste biomass containing acetamido, alcoholic, carbonyl, phenolic, amido and amino groups have been reported to have a high affinity toward heavy metal binding to support these observations [4].

The same functional groups have been identified in raw peel [13] as well, indicating that the main functionalities are not destroyed during NaOH treatment, except deprotonation of acid moieties and cleavage of ester linkages. More importantly, these chemical conversions would enhance the affinity of the biosorbent toward Ni(II). In addition, carboxylic acids, carboxylic acid derivatives (ester and amide) and the phenolic compounds show the affinity for Ni(II) due to the formation of negative ions upon deprotonation.

3.1.2. SEM images

SEM is used to describe the surface morphology of the biosorbent with high resolution and magnification. Further, the elemental composition of the biosorbent can be identified by energy-dispersive X-ray spectroscopy (EDX) coupled with SEM [20,21]. The surface appearance and the dispersion of metals on the surface of the raw peel and STP3, analyzed using SEM images and EDX spectra, are shown in Fig. 2, which indicates the surface inhomogeneity of the sample having particles scattered everywhere without a proper shape (Fig. 2a). However, the surface of STP3 was clear and more orderly, with little cavities identified (marked as circles) in some areas of the image (Fig. 2b). Breaking down of lignin and other molecules in the biosorbent during NaOH treatment would create such cavities, which would contribute to an increase in the surface area. However, the occupation of Ni(II) in the cavities depends on its hydrated radius. The hydrated Ni(II) forms a relatively large structure of octahedral arrangements with water molecules [22], and hence, the occupation of Ni(II) in cavities would not probably be the only mode of mass transfer from the solution phase to the solid biosorbent phase. Surface changes of the biosorbent during NaOH treatment are clear in the EDX spectra recorded showing the disappearance of K peaks after treatment. Replacement of K by Na is thus highly likely. It is also noted that other common metals, such as Mg and Ca, have not changed their peak intensities, indicating their resistance to NaOH treatment.

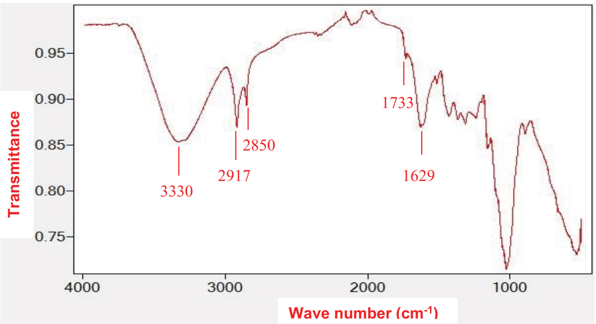

Fig. 1. FTIR spectrum of NaOH-treated peel of *Artocarpus nobilis* fruit (STP3).

Table 1
Active functional groups present in STP3 [13]

Bond type	Wavenumber (cm^{-1})	Functional groups present
C=O		Aldehyde
	1,629	Ester
	1,733	Carboxylic acid
		Amide
O–H	2,850	Alcohol
	2,917	Phenol
	3,330	Carboxylic acids

3.1.3. Specific surface area (SSA) of biosorbent

The plot of amount of MB adsorbed vs. initial concentration ranging from 50.0–2,000.0 mg L^{-1} would lead to the determination of the mass of MB adsorbed at the point of complete cation replacement, which can then be used for the estimation of the specific surface area (SSA) of the biosorbents (DWP and STP3) using Eq. (1) [19],

$$S_S = \frac{m_{\mathrm{MB}} A_v A_{\mathrm{MB}}}{\left(m_S M\right)} \tag{1}$$

where S_S is the surface area of peel (m^2 g^{-1}), m_{MB} is the mass of MB adsorbed at the point of complete replacement (g), A_v is the Avogadro constant (6.022 × 10^{23} mol^{-1}), A_{MB} is the area covered by an MB molecule (130 × 10^{-20} m^2), m_S is the mass of the peel sample (g) and M is the molar mass of MB (319.87 g mol^{-1}). The extent of absorption of MB was performed by changing the initial MB concentrations, and the point of complete MB replacement was obtained as 15.61 and 37.55 mg for DWP and STP3, respectively, which then lead to the SSA of the biosorbents as 381.90 and 919.01 m^2 g^{-1}, respectively. However, the SSA of raw peel cannot be determined using absorbance measurements due to the formation of a pale-colored solution with a raw peel. The SSA of STP3 clearly indicates much increased surface area of the biosorbent in comparison with many other adsorbents [23–25].

3.1.4. XRF analysis

According to the XRF spectrum of raw peel, K, Ge, Cu, Fe and Ca are found to be the major elements present.

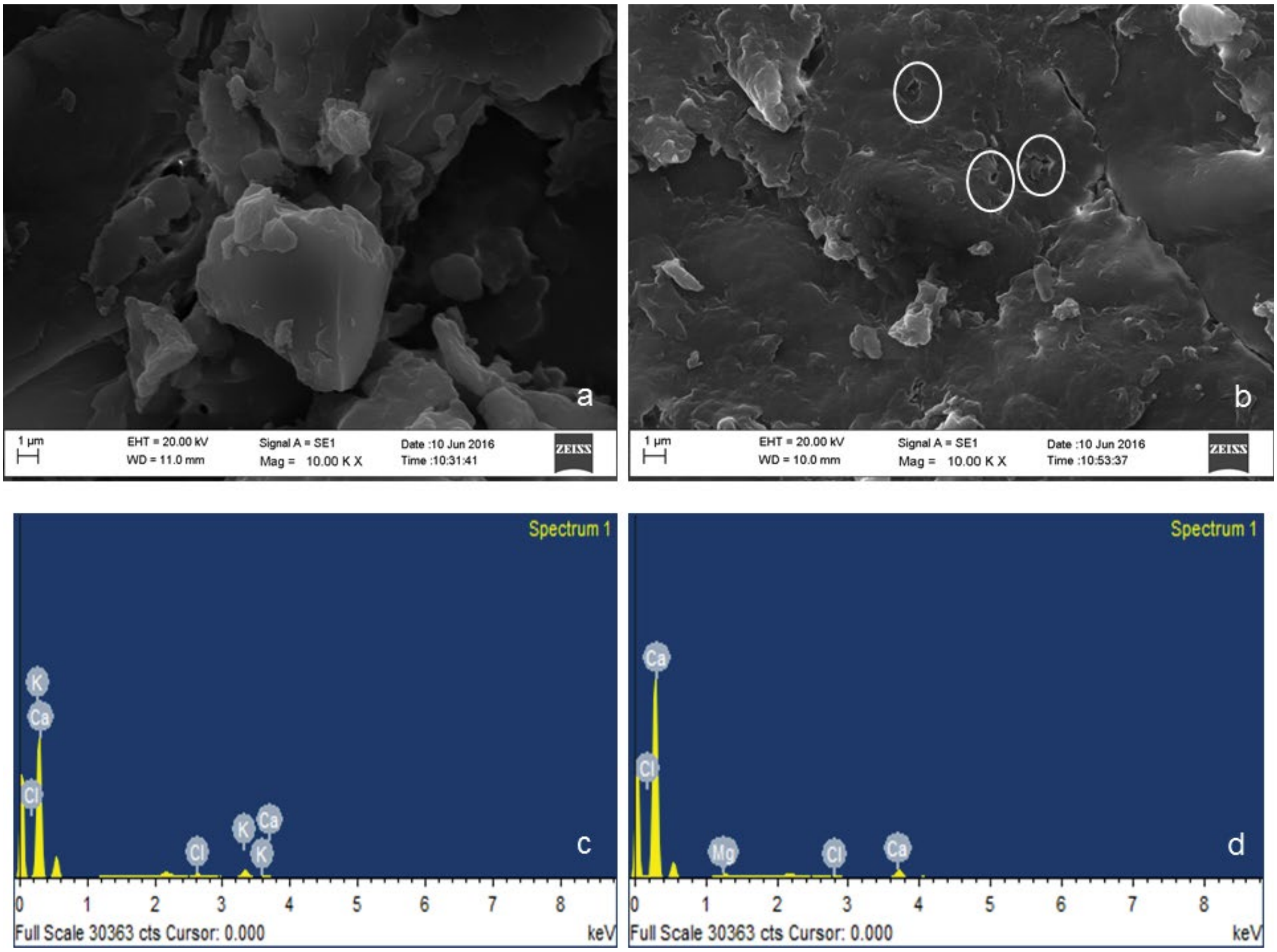

Fig. 2. SEM images of the peel of *Artocarpus nobilis* fruit (a) raw peel and (b) STP3 (magnification 1: 10,000); EDX spectra of (c) raw peel and (d) STP3.

The metal ions available in the soil vary with the soil type, and hence, the composition of the peel depends on the geographical location of the plants. Therefore, the plants are divided into three categories considering the level of accumulation of metal ions, such as excluders, accumulators and indicators [26]. XRF spectra further indicate that metals, such as K and Fe, have leached out when the raw peel is washed with distilled water to form DWP. More importantly, the XRF spectrum of Ni(II)-treated STP3 shows a highly intense peak for Ni, as compared to the spectrum of STP3 which does not show any peak for Ni, providing evidence of biosorption of Ni(II) on a raw peel.

3.1.5. Effect of experimental parameters on the extent of Ni(II) removal

The extents of removal of Ni(II) were determined using 10.0 mg L^{-1} Ni(II) solutions with the mass of 0.100 g of each adsorbent by varying shaking time and immediately separating the biosorbent without allowing any settling time. This dosage was especially selected based on previous results, which is, in fact, a compromise between the extent of removal and the dosage which usually have a positive correlation up to a certain limit [27]. The removal percentages of Ni(II) by DWP, STP1, STP2, STP3 and STP4 thus determined for the above biosorbent dosage were 56%, 69%, 77%, 80% and 84%, respectively, at the saturation limit of 2.0 h, which can be considered as optimum shaking time, beyond which the extent of removal is not much changed (Fig. 3). More importantly, improvement of the extent of removal of Ni(II) upon modification with NaOH solutions is conclusively demonstrated through these observations. The similar variation between the extent of Ni(II) adsorption with shaking time has been observed for the raw peel of *Artocarpus nobilis* fruit leading to the same optimum shaking time, however with much less extent of removal of 45% [13].

According to Fig. 3, the extent of removal of Ni(II) for the biosorbent treated under different conditions show distinct removal capabilities, maintaining the same optimum shaking time, indicating that surface modification has not much influenced the kinetics because the rate of change in the extent of removal during the initial time period of interaction is not much affected by the concentration of the NaOH solution used for modification of the biosorbent. However, adsorption

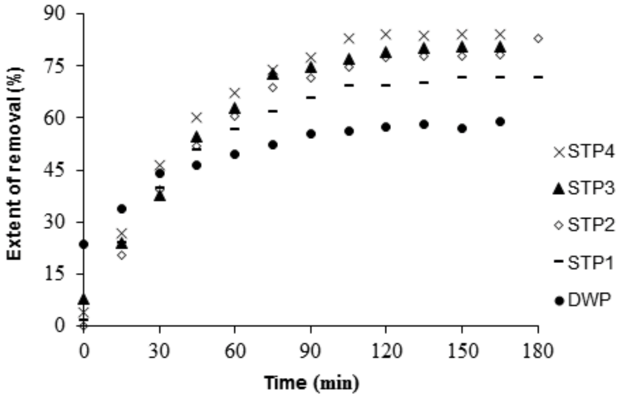

Fig. 3. Variation of extent of removal of Ni(II) with shaking time for DWP, STP1, STP2, STP3 and STP4 (50.0 mL of 10.0 mg L^{-1} Ni(II) solution, 150 rpm, ambient temperature 27°C ± 1°C).

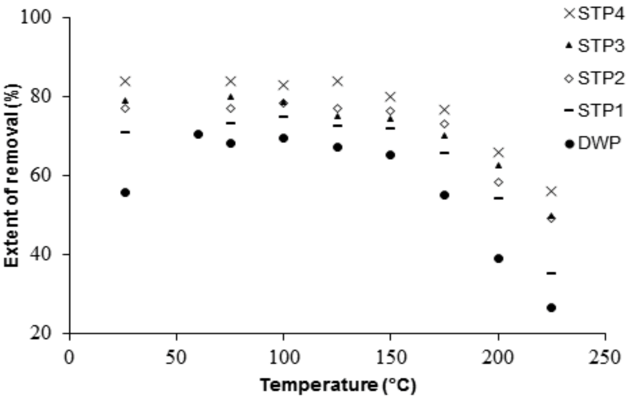

Fig. 4. Variation of extent of removal of Ni(II) with different pretreatment temperatures for DWP, STP1, STP2, STP3 and STP4 (50.0 mL of 10.0 mg L^{-1} Ni(II) solution, 150 rpm, shaking time 2.0 h, settling time 15 min, heating time 15 min, ambient solution temperature 27°C ± 1°C).

equilibrium is affected as noticed by having different saturation limits depending on the concentration of the NaOH solution. This can be explained by considering the enhancement of the porosity and chemical affinity of the biosorbent during modification. Among all, the removal percentage of STP4 was the highest, which is about 30% higher than that of DWP. Other STP types have varying extents of Ni(II) removal depending on the strength of the NaOH solution used.

Then the extent of removal of Ni(II) by DWP, STP1, STP2, STP3 and STP4, determined after allowing the optimum shaking time of 2.0 h, is not much dependent on the settling time and is found to be almost constant from the beginning. Hence, a small settling time of 15 min is considered as optimum to assure the establishment of sorption equilibrium. Similarly, the extent of Ni(II) removal by DWP and STP types is not significantly dependent on the heating time as well at a constant treatment temperature of 125°C. Thus, the minimum period of 15 min was considered as the optimum heating time.

The extent of removal of Ni(II) by DWP and STP samples, determined at optimized shaking, settling and heating times by varying pretreatment temperature of the biosorbent from 27°C ± 1°C (room temperature) to 225°C conducted for all types of modified peels, are shown in Fig. 4. When temperature increases, the chemical and physical properties of the biosorbent would be changed, influencing its adsorption capacities [28,29]. According to the figure, the removal percentage of Ni(II) by DWP was increased with an increase in temperature of treatment of the biosorbent up to 60°C, and thereafter, it was constant up to 125°C, followed by a decrease. On the other hand, the STP types did not show a significant change up to the pre-treatment temperature of 150°C. Further, the extent of biosorption of all types of treated biosorbent was dramatically decreased when the pre-treatment temperature exceeds 150°C. Therefore, the temperature of 75°C was selected as the optimum pre-treatment temperature which leads to 70% Ni(II) removal by DWP. However thermal treatment of STP types is not required. The decomposition of organic substances having functional groups responsible for the interaction of Ni(II) and alteration of the pore structure would be probable reasons for decreasing the extent of removal of Ni(II) at treatment temperatures beyond 125°C [30]. This is further supported by the mass loss observed at higher temperatures recoded in thermal gravimetric analysis curves (Fig. 5).

The extent of removal of Ni(II) by DWP and four types of STP investigated by changing the solution pH from 1.0 to 7.0 under the optimum conditions of shaking time, settling time, heating time and pre-treatment temperature indicates that the percentage removal is not much changed within the pH range from 4.0 to 7.0 (Fig. 6). Low removal percentages recorded below pH 4 would probably be due to the high hindrance of H_3O^+ ions with Ni(II) ions. The sharp increase in Ni(II) removal after pH 3 would be due to less competition of H_3O^+ ions and stronger interaction of Ni(II) with deprotonated carboxylic and phenolic acid groups which is possible after pH 4. It has been reported that carboxylate ions would expose on the peel accelerating metal ion removal efficiencies in the pH range between 4 and 7, supporting the observation made for Ni(II) [31]. The extent of removal is thereafter expected to decrease beyond pH 7 due to the precipitation of $Ni(OH)_2$. The maximum removal efficiency of Ni(II) is expected in the acidic pH range close to 7. Hence, the ambient pH of Ni(II) – DWP and Ni(II) – STP suspensions, which is about 5.0, can be used in biosorption studies without any pH optimization.

3.1.6. Adsorption isotherm experiments

An adsorption isotherm describes the relationship of adsorbate concentration in the bulk and adsorbed amount at the surface of the adsorbent under the equilibrium state [32]. The Langmuir isotherm model assumes the monolayer coverage of biosorbent surface and that the intermolecular forces decrease rapidly with the distance from the adsorption surface, and furthermore, it assumes that all the adsorption sites are energetically identical [33]. The linearized Langmuir isotherm model is given as [34],

$$\frac{C_e}{q_e}=\frac{1}{q_{\max}K_L}+\frac{C_e}{q_m} \tag{2}$$

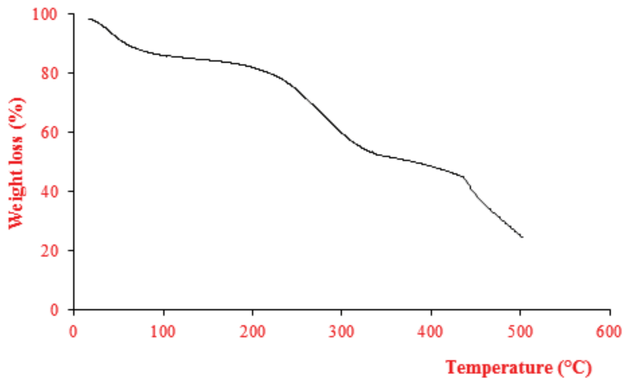

Fig. 5. Thermal gravimetric analysis of raw peel of *Artocarpus nobilis* fruit.

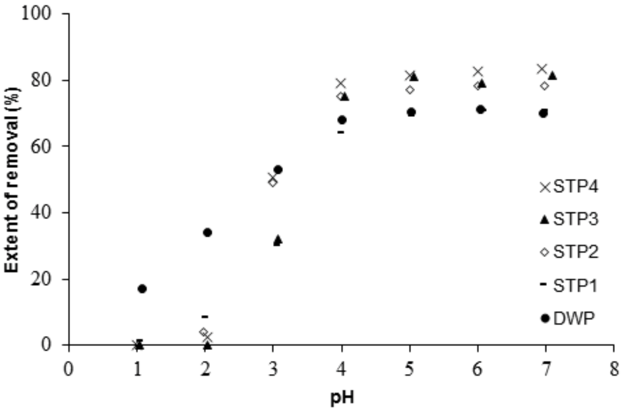

Fig. 6. Variation of extent of removal of Ni(II) with different pH for DWP, STP1, STP2, STP3 and STP4 (50.0 mL of 10.0 mg L^{-1} Ni(II) solution, 150 rpm, shaking time 2.0 h, settling time 15 min, heating time 15 min, pretreatment temperature 75°C for DWP and no thermal treatment for STP, ambient solution temperature 27°C ± 1°C).

where $q_{\max}$ is the maximum monolayer capacity of biosorbent (mg g^{-1}), K_L is the isotherm constant (L mg^{-1}), C_e is the equilibrium concentration of adsorbate (mg L^{-1}) and q_e is the mass adsorbed per unit mass of adsorbent (mg g^{-1}). The Langmuir isotherm model can be used to estimate the equilibrium parameter R_L, a dimensionless constant given in Eq. (3),

$$R_L = \frac{1}{1+\left(1+K_L C_0\right)} \tag{3}$$

where C_0 is the initial concentration (mg L^{-1}) and the value of R_L indicates the adsorption nature; $R_L > 1$ unfavorable adsorption, $R_L = 1$ linear adsorption and $0 < R_L < 1$ favorable adsorption.

On the other hand, the Freundlich adsorption isotherm reveals the heterogeneous adsorption system with multilayer sorption capabilities, and it assumes that binding sites are not equivalent and/or independent. The Freundlich adsorption isotherm model also assumes that the adsorption energy depends on whether the adjacent sites are already occupied or not [2], and the model is expressed as [35],

$$\ln q_e = \ln k_f + \frac{1}{n}\ln C_e \tag{4}$$

where k_f is the Freundlich constant (mg g^{-1}), n is the unitless constant of adsorption intensity, and the $1/n$ is heterogeneity factor which exists in the range from 0–1. If the system is more heterogeneous, the value of $1/n$ is close to zero [36].

Adsorption isotherm experiments performed using Ni(II) solutions within the concentration range of 10–1,000 mg L^{-1} on DWP and STP under optimum experimental conditions reveal that the system under investigation fulfills the requirement of the Langmuir adsorption isotherm more closely than the Freundlich adsorption isotherm, based on regression coefficients (Table 2). As the extent of removal is not much dependent on the pre-treatment temperature of the biosorbent, all isotherm experiments were conducted without any heat treatment.

The adsorption capacity ($q_{\max}$) is increased from STP1 to STP3 and that of the STP4 is little less than the highest $q_{\max}$ (Table 2). Further, the Langmuir constant (K_L) is decreased from STP1 to STP3; however, the K_L of STP4 does not follow the above trend. In addition, the $q_{\max}$ and K_L values of DWP are 13.158 mg g^{-1} and 0.014 L mg^{-1} for the removal of Ni(II). In comparison, the $q_{\max}$ of Ni(II) for raw peel has been reported as 12.048 mg g^{-1} [13].

When compared to raw and DWP, it can be argued that STP type peels show different biosorption capabilities. However, similar adsorption capacities shown by raw peel and STP2 can be explained due to the fact that the strength of the NaOH solution is not sufficient to proceed saponification efficiently, and that some compounds with organic functional groups would be leached out together with enhancing surface area [9]. Both negative and positive effects, when combined, would have matched the adsorption capacity of STP2 to that of raw peel numerically. The negative effect

Table 2
Isotherm constants for the Langmuir and Freundlich adsorption isotherm models for biosorption of Ni(II) on DWP and STP

Type of peel	Model parameters of Langmuir model			
	K_L (L mg^{-1})	$q_{\max}$ (mg g^{-1})	R_L (Avg)	R^2
DWP	0.014	13.158	0.302	0.910
STP1	0.100	7.299	0.118	0.967
STP2	0.098	12.048	0.098	0.991
STP3	0.023	14.925	0.234	0.952
STP4	0.105	14.493	0.091	0.999
	Model parameters of Freundlich model			
	k_f (mg g^{-1})	n	$1/n$	R^2
DWP	1.414	3.008	0.332	0.886
STP1	4.035	9.515	0.105	0.514
STP2	4.018	5.168	0.193	0.835
STP3	3.976	5.405	0.185	0.856
STP4	4.180	4.000	0.250	0.901

of STP1 observed on Ni(II) removal with respect to that of raw peel and DWP is probably due to the fact that Na^+ ions in NaOH are attached to the negative ions on the surface, thus limiting the available adsorption sites for the uptake of Ni(II). On the other hand, slightly decreased adsorption capacity of STP4 could be due to denaturing of the biosorbent as it is prepared with the NaOH solution of the highest concentration.

Therefore, the selection of the best STP type is a crucial factor in this study for accelerated saponification and enhancement of the porous nature. By considering the efficiency of Ni(II) removal, the possibility of denaturing the biosorbent, environmentally friendliness and economical factors, the STP3 is the compromise, as clearly observed in Table 2. The superior nature of DWP and STP types for biosorption of Ni(II) is clear when compared with other low-cost adsorbents as listed in Table 3.

The heavy metal ions in the soluble phase can attract water molecules by the formation of hydrogen bonds according to the ionic radius and the attraction forces. The ionic radius of Ni(II) is comparatively low, and thus, more water molecules can be attracted to the Ni(II) ion. It has been reported that the Ni(II) ion forms octahedral configuration by arranging water molecules around it, thereby increasing the hydrated radius [22]. Fig. 2b shows the small pores on the biosorbent due to the treatment of NaOH, and a significant fraction of the pores would be macropores (>50 nm), mesopores (2–50 nm) and micropores (<2 nm) [7]. Although the SSA of 919.01 $m^2\ g^{-1}$ for STP3 is comparatively larger as compared to that of raw peel and DWP, the maximum adsorption capacity has not improved proportionately, probably due to the occupation of hydrated Ni(II) ions at macropores, limiting their access on mesopores and micropores of STP4.

3.1.7. Kinetics experiments

The biosorption behavior of DWP and STP3 was determined using 10.0 mg L^{-1} of Ni(II) solutions at different contact times. The sampling frequency was arranged as 1 min time intervals for the first 15 min, and thereafter, 5 min intervals up to 60 min for both types of the peel. The data obtained can be applied to PFO and PSO models for investigation of the validity of kinetics behavior of Ni(II) at the interface of the biosorbent. The PFO model is given as [43],

$$\log\left(q_e - q_t\right) = -\frac{k_{11}}{2.303}t + \log\left(q_e\right) \tag{5}$$

where q_e and q_t are the sorption capacity (mg kg^{-1}) at equilibrium and at time t, and k_{11} is the rate constant of PFO sorption (min^{-1}).

If the rate of sorption is a second-order mechanism, the PSO chemisorption kinetics rate equation is expressed as [34],

$$\frac{t}{q_t} = \frac{1}{q_e}t + \frac{1}{k''q_e^2} \tag{6}$$

where q_e and q_t are the sorption capacity at equilibrium and at time t, respectively and k'' is the rate constant of PSO sorption (kg mg^{-1} min^{-1}). The values of relevant parameters calculated using PFO and PSO models are listed in Table 4 for DWP and STP3 biosorbents.

The regression coefficient (R^2) of the kinetics models represent the validity of the model, and according to Table 4, the PFO shows higher R^2 values as compared to those of the PSO model for both types of peel, and hence, the latter model should not be considered in the interpretation of results. The rate constant determined from the PFO model increases from 3.87×10^{-2} to 6.70×10^{-2} min^{-1} for DWP and STP3, respectively, further supporting the superior behavior of STP to DWP, as explained earlier.

3.1.8. IPD model

The kinetics data related to the extent of removal of Ni(II) with DWP and STP3 can be applied to the IPD model for identification of diffusion behavior of Ni(II) ions on the biosorbent surface. This model is expressed as [44],

$$q_e = k_p t^{1/2} + C \tag{7}$$

where q_e is the amount adsorbed (mg kg^{-1}) at time t (min), k_p is the IPD rate constant (mg kg^{-1} $min^{-1/2}$) and C is a constant for a given adsorbate-adsorbent system under a given set of experimental conditions (mg kg^{-1}). A positive value of C indicates rapid adsorption in short time periods, while a negative value of C indicates the boundary layer retarded IPD [45]. The variation of q_e of Ni(II) against the $t^{1/2}$ is shown in Fig. 7.

Fig. 7 shows that three trend lines of different slopes are present for both DWP and STP3. This is a clear indication that biosorption occurs in three stages: (1) Rapid diffusion of Ni(II) ions onto the surface of biosorbents; (2) IPD which could be the rate-limiting step; and (3) establishment

Table 3
Variation of maximum adsorption capacity of DWP and STP with low-cost adsorbents for Ni(II)

Adsorbent	Adsorption capacity (mg g^{-1})	Reference
Modified rice straw (amine treated)	6.23	[37]
Coconut copra meal (HCl treated)	3.77	[38]
Moringa aptera Gaertn (heat-treated)	5.53	[39]
Sugarcane bagasse	2.23	[40]
Cystoseira indica-brown algae (formaldehyde-treated)	10.06	[41]
Rice husk (alkali treatment)	5.52	[42]

of equilibrium. Therefore, the constants of the IPD model, k_p and C, were calculated using the second linear portion of Fig. 7 (Table 5).

The regression coefficients for both DWP and STP3, being very close to unity, conclusively demonstrates that adsorption of Ni(II) on both adsorbent types follows the IPD model (Table 5). The intercept C is indicative of the boundary layer thickness and that can be determined by extrapolating the linear portion of the graph (denoted as q_e). According to Table 5, the positive sign of C for Ni(II)/STP3 system is evident in favorable conditions for biosorption, as evidenced throughout this work. Nevertheless, the negative sign of C obtained for DWP is indicative of a barrier for biosorption of Ni(II). Based on the IPD model, the value of C represents the initial adsorption amount, and therefore, C can be used to describe the initial kinetics behavior of the adsorption system.

3.2. Biosorption mechanism

The fruit peel of *Artocarpus nobilis* is a biosorbent comprising acidic organic functional groups. After the modification process, the porous nature of the biosorbent is enhanced. According to regression analysis, the Langmuir isotherm is the best-fitted model at Ni(II) concentrations under investigation, and it describes the monolayer biosorption, which is probably followed by multilayer biosorption at higher Ni(II) concentrations. However, the filling of macropores, mesopores and micropores of the biosorbent by Ni(II) is a time-dependent processes, influenced by some physical and chemical factors. A schematic diagram of the biosorption mechanism is shown in Fig. 8.

4. Conclusion

The fruit peel of *Artocarpus nobilis* is an efficient biosorbent for the removal of Ni(II) from synthetic effluents. This natural material can easily be modified with aqueous NaOH solutions. Under the optimum conditions, the adsorption capacities vary between 7,299 and 14,925 mg kg^{-1} in STP type peels, while DWP shows the capacity of 13,158 mg kg^{-1}.

Table 5
Variations of parameters of IPD model for DWP and STP3

Types of peel	k_p (mg kg^{-1} $min^{-1/2}$)	C (mg kg^{-1})	R^2
DWP	457.06	–363.7	0.999
STP3	367.31	+164.4	0.993

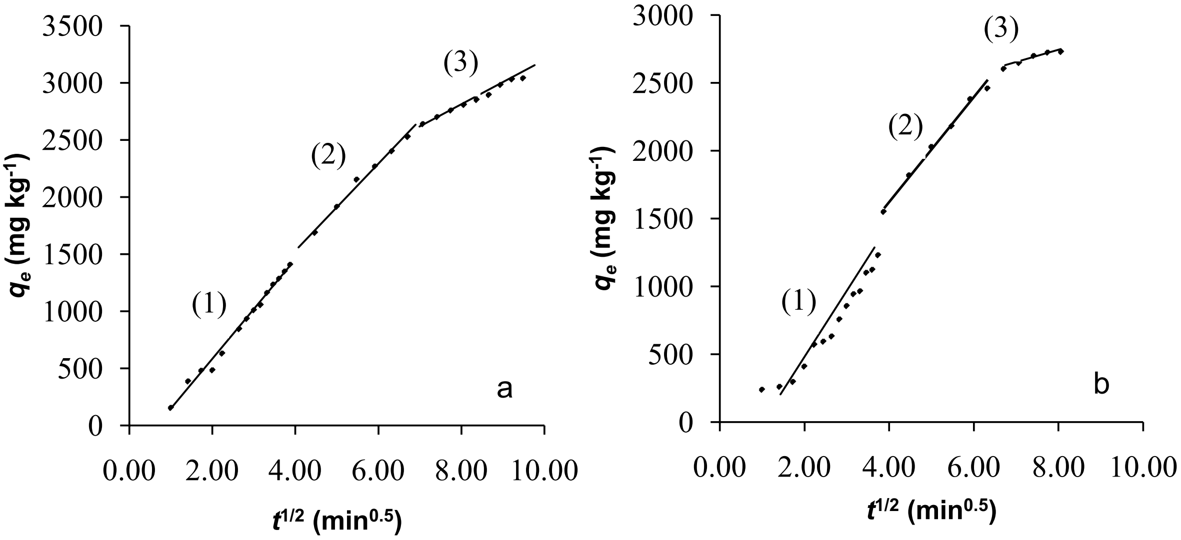

Fig. 7. Application of IPD model for the extent of removal of Ni(II) with (a) DWP and (b) STP3 (10.0 mg L^{-1} of Ni(II) solution, ambient temperature 27°C ± 1°C).

Table 4
Application of kinetics models for the removal of Ni(II) with different types of peel of *Artocarpus nobilis*

Kinetic model	Parameter	Type of peel	
		DWP	STP3
Pseudo-first-order model (PFO)	k_{11} (min^{-1})	3.87×10^{-2}	6.70×10^{-2}
	R^2	0.998	0.978
Pseudo-second-order model (PSO)	k'' (kg mg^{-1} min^{-1})	1.07×10^{-5}	6.43×10^{-6}
	R^2	0.993	0.928

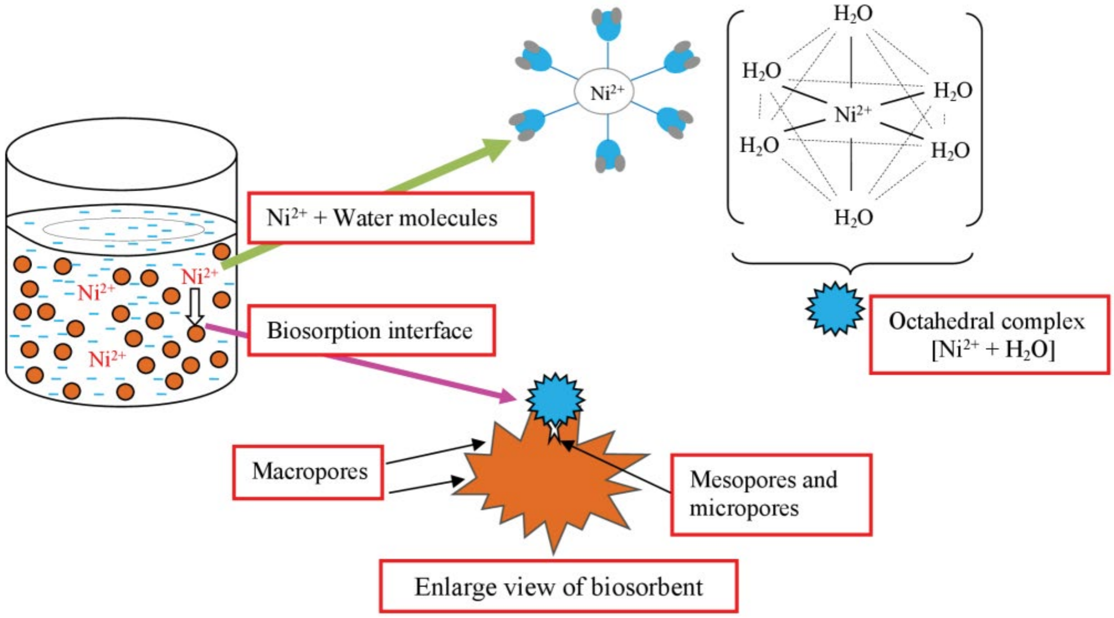

Fig. 8. Schematic diagram of the biosorption mechanism of the peel of *Artocarpus nobilis* fruit with Ni(II).

In addition, the surface area of DWP (381.9 $m^2 g^{-1}$) has been increased up to 919.0 $m^2 g^{-1}$ through modification with 0.10 M NaOH, which is a great achievement. This surface area enhancement is evidenced by SEM images, which clearly show small cavities on STP type peel, which is attributed to cleavage of ester linkages and ionization of acidic functional groups. The extent of removal of Ni(II) with DWP, STP1, STP2, STP3, and STP4 is recorded as 56%, 69%, 77%, 80%, and 84%, respectively, at the optimum shaking and settling times, and at ambient solution pH of about 5.0. Further, biosorption of Ni(II) by DWP and STP3 fulfills the requirements of the PFO model. More importantly, Ni(II)/STP3 system demonstrates favorable conditions for biosorption, although there is a barrier for biosorption of Ni(II) on DWP according to the IPD model. The investigation of metal ions with smaller hydrated radii would be the next logical continuation of this research.

References

[1] P. Haynes, Complexity theory and evaluation in public management, Public Manage. Rev., 10 (2008) 401–419.

[2] K.A. Shroff, V.K. Vaidya, Kinetics and equilibrium studies on biosorption of nickel from aqueous solution by dead fungal biomass of *Mucor hiemalis*, Chem. Eng. J., 171 (2011) 1234–1245.

[3] Z. Li, Z. Ma, T.J. van der Kuijp, Z. Yuan, L. Huang, A review of soil heavy metal pollution from mines in China: pollution and health risk assessment, Sci. Total Environ., 468–469 (2014) 843–853.

[4] D. Sud, G. Mahajan, M. Kaur, Agricultural waste material as potential adsorbent for sequestering heavy metal ions from aqueous solutions – a review, Bioresour. Technol., 99 (2008) 6017–6027.

[5] A. Saravanan, P.S. Kumar, M. Yashwanthraj, Sequestration of toxic Cr (VI) ions from industrial wastewater using waste biomass: a review, Desal. Wat. Treat., 68 (2017) 245–266.

[6] WHO, Guidelines for Drinking-Water Quality, World Health Organization, Geneva, Switzerland, 2011.

[7] M. Thommes, K. Kaneko, A.V. Neimark, J.P. Olivier, F. Rodriguez-Reinoso, J. Rouquerol, K.S.W. Sing, Physisorption of gases, with special reference to the evaluation of surface area and pore size distribution (IUPAC Technical Report), Pure Appl. Chem., 87 (2015), doi: https://doi.org/10.1515/pac-2014-1117.

[8] Y. Sun, J. Cheng, Hydrolysis of lignocellulosic materials for ethanol production: a review, Bioresour. Technol., 83 (2002) 1–11.

[9] W.S. Wan Ngah, M.A.K.M. Hanafiah, Removal of heavy metal ions from wastewater by chemically modified plant wastes as adsorbents: a review, Bioresour. Technol., 99 (2008) 3935–3948.

[10] A.A. Abia, E.D. Asuquo, Lead(II) and nickel(II) adsorption kinetics from aqueous metal solutions using chemically modified and unmodified agricultural adsorbents, Afr. J. Biotechnol., 5 (2006) 1475–1482.

[11] S.H. Min, J.S. Han, E.W. Shin, J.K. Park, Improvement of cadmium ion removal by base treatment of juniper fiber, Water Res., 38 (2004) 1289–1295.

[12] F.A. Chowdhury, M. Azizur Raman, A. Jabbar Mian, Distribution of free sugars and fatty acids in jackfruit (*Artocarpus heterophyllus*), Food Chem., 60 (1997) 25–28.

[13] N. Priyantha, P.A. Kotabewatta, Biosorption of heavy metal ions on peel of *Artocarpus nobilis* fruit: 1—Ni(II) sorption under static and dynamic conditions, Appl. Water Sci., 9 (2019) 1–10.

[14] U. Farooq, J.A. Kozinski, M.A. Khan, M. Athar, Biosorption of heavy metal ions using wheat based biosorbents – a review of the recent literature, Bioresour. Technol., 101 (2010) 5043–5053.

[15] K. Harsha, P. Senthil, R.C. Panda, A review on heavy metal pollution, toxicity and remedial measures : current trends and future perspectives, J. Mol. Liq., 290 (2019) 111197.

[16] A.K. Meena, K. Kadirvelu, G.K. Mishra, C. Rajagopal, P.N. Nagar, Adsorptive removal of heavy metals from aqueous solution by treated sawdust (*Acacia arabica*), J. Hazard. Mater., 150 (2008) 604–611.

[17] D.K.V. Ramana, D.H.K. Reddy, B.N. Kumar, Y. Harinath, K. Seshaiah, Removal of nickel from aqueous solutions by citric acid modified *Ceiba pentandra* hulls: equilibrium and kinetic studies, Can. J. Chem. Eng., 90 (2012) 111–119.

[18] M. Kazemipour, M. Ansari, S. Tajrobehkar, Removal of lead, cadmium, zinc, and copper from industrial wastewater by carbon developed from walnut, hazelnut, almond, pistachio shell, and apricot stone, J. Hazard. Mater., 150 (2008) 322–327.

[19] Y. Yukselen, A. Kaya, Suitability of the methylene blue test for surface area, cation exchange capacity and swell potential determination of clayey soils, Eng. Geol., 102 (2008) 38–45.

[20] M.B. Shakoor, N.K. Niazi, I. Bibi, M. Shahid, M. Farrakh, S.M. Shaheen, H. Wang, D.C.W. Tsang, J. Bundschuh, Y. Sik, J. Rinklebe, Exploring the arsenic removal potential of various biosorbents from water, Environ. Int., 123 (2019) 567–579.

[21] Z. Cheng, A. Lai, K. Tan, Y. Tao, D. Shan, K.E. Ting, X.J. Yin, Synthesis and characterization of iron oxide nanoparticles and applications in the removal of heavy metals from industrial wastewater, Int. J. Photoenergy, 2012 (2012) 5.

[22] I. Persson, Hydrated metal ions in aqueous solution: how regular are their structures?, Pure Appl. Chem., 82 (2010) 1901–1917.

[23] B. Inbaraj, Carbonised jackfruit peel as an adsorbent for the removal of Cd(II) from aqueous solution, Bioresour. Technol., 94 (2004) 49–52.

[24] C.H. Weng, Y.T. Lin, T.W. Tzeng, Removal of methylene blue from aqueous solution by adsorption onto pineapple leaf powder, J. Hazard. Mater., 170 (2009) 417–424.

[25] E.I. Unuabonah, G.U. Adie, L.O. Onah, O.G. Adeyemi, Multistage optimization of the adsorption of methylene blue dye onto defatted *Carica papaya* seeds, Chem. Eng. J., 155 (2009) 567–579.

[26] J.R. Peralta-videa, M. Laura, M. Narayan, G. Saupe, J. Gardea-torresdey, The biochemistry of environmental heavy metal uptake by plants: implications for the food chain, Int. J. Biochem. Cell Biol., 41 (2009) 1665–1677.

[27] N.P. Raval, P.U. Shah, N.K. Shah, Adsorptive removal of nickel (II) ions from aqueous environment: a review, J. Environ. Manage., 179 (2016) 1–20.

[28] A. Sen, H. Pereira, M.A. Olivella, I. Villaescusa, Heavy metals removal in aqueous environments using bark as a biosorbent, Int. J. Environ. Sci. Technol., 12 (2015) 391–404.

[29] H. Li, X. Dong, B. Evandro, L.M. De Oliveira, Y. Chen, L.Q. Ma, Mechanisms of metal sorption by biochars: biochar characteristics and modifications, Chemosphere, 178 (2017) 466–478.

[30] E. Pehlivan, T. Altun, Modified barley straw as a potential biosorbent for removal of copper ions from aqueous solution, Food Chem., 135 (2012) 2229–2234.

[31] A. Kurniawan, A.N. Kosasih, J. Febrianto, Y.-H. Ju, J. Sunarso, N. Indraswati, S. Ismadji, Evaluation of cassava peel waste as lowcost biosorbent for Ni-sorption: equilibrium, kinetics, thermodynamics and mechanism, Chem. Eng. J., 172 (2011) 158–166.

[32] A. Demirbas, Heavy metal adsorption onto agro-based waste materials: a review, J. Hazard. Mater., 157 (2008) 220–229.

[33] N. Unlu, M. Ersoz, Adsorption characteristics of heavy metal ions onto a low-cost biopolymeric sorbent from aqueous solutions, J. Hazard. Mater., 136 (2006) 272–280.

[34] L.B.L. Lim, N. Priyantha, C. Hei Ing, M. Khairud Dahri, D.T.B. Tennakoon, T. Zehra, M. Suklueng, *Artocarpus odoratissimus* skin as a potential low-cost biosorbent for the removal of methylene blue and methyl violet 2B, Desal. Wat. Treat., 53 (2015) 964–975.

[35] H.I. Chieng, L.B.L. Lim, N. Priyantha, Sorption characteristics of peat from Brunei Darussalam for the removal of rhodamine B dye from aqueous solution: adsorption isotherms, thermodynamics, kinetics and regeneration studies, Desal. Wat. Treat., 55 (2015) 664–677.

[36] F. Haghseresht, G.Q. Lu, Adsorption characteristics of Phenolic compounds onto coal-reject-derived adsorbents, Energ. Fuel, 12 (1998) 1100–1107.

[37] Y. Wu, Y. Fan, M. Zhang, Z. Ming, S. Yang, A. Arkin, Functionalized agricultural biomass as a low-cost adsorbent: utilization of rice straw incorporated with amine groups for the adsorption of Cr(VI) and Ni(II) from single and binary systems, Biochem. Eng. J., 105 (2016) 27–35.

[38] M. Saleem, N. Wongsrisujarit, S. Boonyarattanakalin, Removal of nickel(II) ion by adsorption on coconut copra meal biosorbent, Desal. Wat. Treat., 57 (2016) 5623–5635.

[39] M. Matouq, N. Jildeh, M. Qtaishat, M. Hindiyeh, M.Q. Al, The adsorption kinetics and modeling for heavy metals removal from wastewater by *Moringa* pods, J. Environ. Chem. Eng., 3 (2015) 775–784.

[40] M. Alomá, M.A. Martín-Lara, I.L. Rodríguez, G. Blázquez, M. Calero, Removal of nickel (II) ions from aqueous solutions by biosorption on sugarcane bagasse, J. Taiwan Inst. Chem. Eng., 43 (2012) 275–281.

[41] M.M. Montazer-rahmati, P. Rabbani, A. Abdolali, A. Reza, Kinetics and equilibrium studies on biosorption of cadmium, lead, and nickel ions from aqueous solutions by intact and chemically modified brown algae, J. Hazard. Mater., 185 (2011) 401–407.

[42] K.K. Krishnani, X. Meng, C. Christodoulatos, V.M. Boddu, Biosorption mechanism of nine different heavy metals onto biomatrix from rice husk, J. Hazard. Mater., 153 (2008) 1222–1234.

[43] C.C.V. Cruz, A.C.A. da Costa, C.A. Henriques, A.S. Luna, Kinetic modeling and equilibrium studies during cadmium biosorption by dead *Sargassum* sp. biomass, Bioresour. Technol., 91 (2004) 249–257.

[44] F. Wu, R. Tseng, R. Juang, Initial behavior of intraparticle diffusion model used in the description of adsorption kinetics, Chem. Eng. J., 153 (2009) 1–8.

[45] T.M. Ting, M.M. Nasef, K. Hashim, Evaluation of boron adsorption on new radiation grafted fibrous adsorbent containing N-methyl-D-glucamine, J. Chem. Technol. Biotechnol., 91 (2016) 2009–2017.